Journal of Physical and Theoretical Chemistry
of Islamic Azad University of Iran, 12 (2) 121-136: Summer 2015
(J. Phys. Theor. Chem. IAU Iran)
ISSN 1735-2126

A quantum-mechanical study on nitro and amino derivatives of 1,2,3,4-tetrazine

Mehdi Nabati* and Mehrdad Mahkam

Chemistry Department, Faculty of Science, Azarbaijan Shahid Madani University, Tabriz, Iran

Received March 2015; Accepted May 2015

ABSTRACT

In the present study, all possible nitro and amino-substituted 1,2,3,4-tetrazine molecules have been investigated as potential candidates for high energy density materials (HEDMs) by using quantum chemical treatment. All compounds were designed and optimized to obtain molecular geometries and electronic structures at ab-initio and density functional theory (DFT, B3LYP) at the levels of 6-31G(d,p), 6-31+G(d,p), 6-311G(d,p), 6-311+G(d,p) and cc-pvDZ. Moreover, thermal stabilities have been evaluated from the hemolytic bond dissociation energies (BDEs). Other important properties such as bond dissociation density, frontier orbital energy, nucleus-independent chemical shifts (NICSs), and heat of formation and detonation parameters were then calculated. Also, IR and NMR spectra of the structures were obtained. According to the results of the calculations, the introduction of nitro group can improve the detonation properties of the structures. The calculation results revealed that these molecules exhibit excellent performance; and the all compounds are viable candidate of high energy density materials (HEDMs). Comparing the detonation properties of molecules with standards (RDX and HMX) shows 5,6-dinitro-1,2,3,4-tetrazine can be an explosive.

Keywords: 1,2,3,4-tetrazine; Nitrogen-rich compounds; Bond dissociation energy; Heat of formation; Detonation properties

INTRODUCTION

Energetic materials research encompassing all propellants, explosives, and pyrotechnics has long attracted intense work in the chemical sciences, with participating scientists including Liebig, Berzelius, and Gay-Lussac [1]. This tradition has led to many chemical advances. For example, work with silver fulminate, which has the same composition as silver cyanate, led to the concept of isomerism. Studies of unstable compounds on the borderline of existence and nonexistence allow elucidation of the fundamental properties affecting chemical stability and bonding [2, 3]. The concept of new class of high nitrogen content high energy materials (HNC-HEMs) has evinced great interest during recent time as an energetic component of propellants. Presence of N–N and C–N bonds in HNC compounds confers positive heat of formation on them. Further, HNC-HEMs produce more nitrogen gas per gram than most of the HEMs, resulting in inherently

---

*Corresponding author: mnabati@ymail.com

cooler combustion products, which is an attractive feature for gun propellants and gas generators. Low percentage of carbon and hydrogen in these compounds reduces the proportion of oxidized combustion products in comparison to conventional HEMs, resulting in formation of low mean molecular weight combustion products like methane. These compounds are reported to have a combination of high positive heat of formation and insensitivity [4, 5]. The six-membered heterocycle consisting of four nitrogen atoms and two carbon atoms is known as the tetrazine ring system. Tetrazines belong to a class of molecules that are found to be useful in various sectors as drugs, explosives and sensors. The 1,2,3,4-tetrazine and its' derivatives weren't synthesized nowadays [6]. A particularly important method is to model a molecular system prior to synthesizing that molecule in the laboratory. This is very useful mean because synthesizing a compound could need months of labor and raw materials, and generates toxic waste [7]. A second use of computational chemistry is in understanding a problem more completely [8]. There are some properties of a molecule that can be obtained theoretically more easily than by experimental means [9]. Density functional theory (DFT) has become very popular in recent years. This is justified based on the pragmatic observation that it is less computationally intensive than other methods with similar accuracy. This theory has been developed more recently than other ab-initio methods [10, 11]. In this paper, stabilities of six structures as potential candidates for high energy density materials (HEDMs) have been investigated theoretically by using quantum chemical treatment. Geometric features, electronic structures of these tetrazine derivatives have been systematically studied using ab-initio and density functional theory (DFT, B3LYP) at the level of 6-31G(d,p), 6-31+G(d,p), 6-311G(d,p), 6-311+G(d,p), cc-pvDZ. Moreover, these molecules properties were investigated at B3LYP/6-311G (d,p) level.

COMPUTATIONAL METHODS

In this work, we study theoretically the structural and energetically properties of nitro and amino organic compounds based on 1,2,3,4-tetrazine system with positive and negative variances of their surface electrostatic potentials. All calculations were carried out with the Gaussian 03 package [12] using the spin-restricted Hartree-Fock (RHF) and the B3LYP methods with 6-31G(d,p), 6-31+G(d,p), 6-311G(d,p), 6-311+G(d,p) and cc-pvDZ basis sets. All calculations and geometry optimization for each molecule were obtained the mentioned theories (RHF and B3LYP). The term of B3LYP consists of the Vosko, Wilk, Nusair (VWN3) local correlation functional [13] and the Lee, Yang, Parr (LYP) correlation correction functional [14,15]. For comparing of the bond strengths, homolytic bond dissociation energy (BDE) calculations were performed by B3LYP/6-311G(d,p) level. The mentioned level was used to predict the HOFs of all molecules via isodesmic reactions. Vibrational analyses without any symmetry constraints were done for each set of calculations by the same basis set. Theoretical calculations have been performed in the gas phase [16, 17]. The restricted method was used for the systems. An efficient and convenient statistics average method was worked out to predict the crystalline densities of all derivatives. To calculate the densities of structures, the molecular volume data was required. The molecular volume V was defined as inside a contour of 0.001 electrons/bohr^3 density. The computational molecular density ρ (ρ=M/V, where M = molecular weight) was also calculated. Oxygen balance (OB_{100}) is an expression that is used to indicate the degree to which an explosive can be oxidized. OB_{100} was calculated as follows:

$$OB\% = \frac{-1600}{Mol.wt} \times \left(2a + \frac{b}{2} - c\right) \qquad (1)$$

where, a = number of atoms of carbon, b = number of atoms of hydrogen, c = number of atoms of oxygen.

RESULTS AND DISCUSSION

The geometries of interested molecules

The studied six molecules are 1,2,3,4-tetrazine (A), 5-amino-1,2,3,4-tetrazine (B), 5,6-diamino-1,2,3,4-tetrazine (C), 5-nitro-1,2,3,4-tetrazine (D), 5,6-dinitro-1,2,3,4-tetrazine (E) and 5-amino-6-nitro-1,2,3,4-tetrazine (F). The molecular frameworks of six title compounds are displayed in Figure 1. The chemical structures and atomic numbering of the compounds are shown in Figure 2. The geometric structures of the molecules with electron charge of the elements of each compound are shown in Figure 3. The dipole moments of the molecules are listed in Table 1. As seen from the table, the μ order is C□B□F□A>D>E for the structures at B3LYP/6-311G(d,p) level of theory. It is obtained that dipole moment increases by nitro groups.

Bond lengths, Bond Angles and Dihedral Angles

The bond lengths data of the molecules have been given in Table 2. It is obtained that the N3-N4 bond length decreases by introduction of amino and nitro groups. Also the C1-C6 bond length increase by introduction of amino group and decreases by introduction of nitro group. From data, it is observed that the C-NH_2 bond length is shorter than C-NO_2 bond length in the F structure as expected due to the electron donating and electron withdrawing characters of the groups. And also N-H and N-O bonds decrease in nitro and amino derivatives respectively. The molecular electrostatic potential (MEP) is the force acting on a positive test charge (a proton) located at a given point in the vicinity of a molecule through the electrical charge cloud generated through the molecules electrons and nuclei [18, 19]. The three-dimensional electrostatic potential maps of the structures are shown in Figure 4. The red loops and the blue loops indicate negative and positive charge development for a particular system respectively. As can be seen from the figures the negative charge is located on the nitrogen elements of the tetrazine ring and the nitro groups as expected due to the electron withdrawing character of theirs and positive charge is located on the amino groups as expected due to the electron donating character of amino groups in the structure. However, charge development on nitrogen elements of rings decreases with increasing number of nitro groups in the structure and also it increases with increasing number of amino groups in the structure.

The bond angles data of the molecules have been given in Tables 3 and 4. From data, it is obtained that the amino group decrease O-N-O angle and nitro group increase H-N-H angle. The dihedral angles of structures show us that all of the structures aren't planar.

Nucleus Independent Chemical Shifts (NICS)

Aromaticity continues to be an actively investigated area of chemistry. In 1996, Schleyer has proposed the use of absolute magnetic shieldings, computed at ring centers (nonweighted mean of the heavy atom coordinates) with available quantum mechanics programs, as a new aromaticity /antiaromaticity criterion [20].

The B3LYP/6-311G(d,p) level by gauge invariant atomic orbital (GIAO) approach was used for nucleus independent chemical shift (NICS) calculations at the center of rings. To correspond to the familiar NMR chemical shift convention, the signs of the computed values are reversed: Negative "nucleus-independent chemical shifts" (NICSs) denote aromaticity; positive NICSs, antiaromaticity; small NICS, non-aromaticity. In this study, NICS values of the tetrazine derivatives have been calculated by the application of density functional theory using the standard 6-311G(d,p) basis set (Table 5). Nitro derivatives of tetrazine (D, E) have been found to be aromatic but other structures (A, B and C) have been found to be non-aromatic. Nitrogen atoms in the rings are higher electronegativity than carbon atoms and for this reason, the electrons located on the nitrogen atoms. In the D, E and F structures, the electrons have been pulled into the rings by the attachment of very strongly withdrawing nitro groups.

Infrared spectra

The IR spectrum is one basic property of a compound, and also an effective measure to identify structures. Here, vibrational frequencies were calculated by using the B3LYP/6-311G (d,p) level. Figure 5 provides structures' IR spectra.

Harmonic frequencies (cm^{-1}), IR intensities (KM/Mole)

A: 305.54 (6.36), 651.49 (0.11), 725.64 (1.45), 812.45 (0.07), 877.2 (6.04), 1030.8 (1.54), 1075.74 (16.91), 1120.56 (2.31), 1141.3 (0.72), 1325.43 (12.85), 1365.18 (0.036), 1548.08 (13.19), 1574.5 (8.1), 3163.78 (1.31), 3179.31 (11.34).

B: 71.34 (195.3), 137.52 (14.39), 347.25 (5.72), 368.03 (2.31), 490.43 (4.83), 574.75 (12.48), 589.56 (0.39), 681.79 (0.15), 808.01 (0.92), 841.7 (9.44), 915.16 (7.56), 940.53 (2.24), 1032.6 (0.0024), 1068.2 (15.88), 1094.93 (22.89), 1238.77 (20.93), 1349.05 (21.09), 1447.89 (56.36), 1522.19 (18.87), 1587.96 (42.2), 1653.22 (332.72), 3138.65 (15.91), 3599.16 (91.77), 3731.87 (56.8).

C: 134.22 (0.12), 283.59 (0.0018), 287.63 (0.61), 312.5 (13.97), 429.25 (32.13), 461.8 (0.45), 511.56 (64.27), 561.28 (8.36), 618 (114.24), 641.46 (0.015), 678.75 (269.37), 692.48 (163.75), 755.93 (0.27), 806.39 (16.07), 992.2 (9.04), 1003.08 (0.025), 1061.55 (14.94), 1068.56 (0.037), 1207.48 (2.85), 1246.96 (31.13), 1342.52 (21.63), 1480.83 (188.8), 1542.09 (32.99), 1590.57 (61.69), 1647.68 (148.36), 1649.4 (161.71), 3535.43 (39.69), 3537.74 (25.66), 3640.62 (52.21), 3643.59 (19.94).

D: 8.69 (1.04), 115.49 (11.6), 234.13 (5.54), 313.21 (3.19), 376.06 (0.92), 381.57 (9.95), 519.92 (1.4), 661.8 (0.29), 739.06 (1.44), 759.65 (12.22), 806.59 (25.32), 809.48 (0.37), 895.53 (24.86), 971.3 (4.15), 1052.95 (2.55), 1069.65 (19.68), 1162.68 (1.84), 1241.01 (5.11), 1325.99 (11.88), 1373.96 (120.63), 1521.82 (25.63), 1577.21 (17.5), 1672.67 (227.41), 3216.22 (3.75).

E: 29.14 (0.05), 68.96 (0.11), 82.25 (0.037), 147.51 (0.73), 171.82 (10.84), 267.08 (7.99), 311.6 (0.73), 317.66 (0.62), 346.81 (10.84), 399.06 (4.65), 592.51 (2.99), 607.39 (0.27), 674.72 (0.23), 742.43 (0.43), 757.97 (1.6), 774.28 (38.14), 807.15 (9.58), 829.33 (10.69), 889.31 (36.12), 912.28 (16.27), 1096.08 (0.01), 1132.4 (18.27), 1199.03 (2.59), 1310.42 (21.49), 1377.2 (78.96), 1389.83 (157.14), 1509.79 (10.96), 1552.29 (0.01), 1667.21 (499.88), 1671.14 (20.79).

F: 38.62 (0.03), 85.61 (2.93), 247.91 (1.89), 263.52 (6.93), 364.76 (1.22), 375.42 (5.87), 388.62 (6.91), 456.06 (214.07), 539.46 (6.08), 579.8 (5.19), 610.17 (0.94), 660.48 (0.11), 711.8 (0.27), 744.44 (0.95), 800.26 (4.28), 823.77 (147.69), 860.56 (7.13), 961.35 (1.99), 1049.9 (6.83), 1130.94 (6.47), 1167.6

(0.93), 1324.82 (63.24), 1344.37 (135.19), 1438.72 (35.63), 1469.03 (2.08), 1549.82 (62.38), 1650.24 (26.21), 1673.59 (581.6), 3558.34 (112.14), 3695.16 (120.16).

NMR study

The NMR analysis is an important property of a compound, and also an effective measure to identify structures. Here, the nucleus shielding (ppm) for the structures were calculated by using B3LYP/6-311G (d,p) level of theory.

A: -259.252 (N4), -259.251 (N5), -183.310 (N2, N3), 23.042 (H7, H8), 36.817 (C1, C6).

B: -246.241 (N3), -206.568 (N4), -174.869 (N5), -116.932 (N2), 23.641 (H8), 27.535 (H9), 28.339 (H10), 32.219 (C1), 49.444 (C6), 184.943 (N8).

C: -214.239 (N3), -214.238 (N4), -113.108 (N2, N5), 28.064 (H9, H11), 28.881 (H10, H12), 36.687 (C1, C6), 192.335 (N7, N8).

D: -356.303 (O9), -327.102 (O10), -280.36 (N4), -256.236 (N3), -201.841 (N5), -154.035 (N2), -128.71 (N7), 22.105 (H8), 27.349 (C1), 44.228 (C6).

E: -380.429 (O9, O11), -375.248 (O10), -375.247 (O12), -272.623 (N3, N4), -164.616 (N2, N5), -128.227 (N7, N8), 30.943 (C1, C6).

F: -364.553 (O9), -310.083 (O10), -283.863 (N4), -206.988 (N3), -153.992 (N5), -149.441 (N2), -139.706 (N7), 24.184 (H11), 26.463 (H12), 37.072 (C1), 37.102 (C6), 165.954 (N8).

Energies of structures

Tables 6 and 7 show the calculated total energies of the structures at spin- restricted Hartree-Fock (RHF) level and density functional theory (DFT, B3LYP) at the 6-31G(d,p), 6-31+G(d,p), 6-311G(d,p), 6-311+G(d,p), cc-pvDZ basis sets, respectively. Total energies are corrected for zero-point vibrational energy (ZPVE). As seen from the tables, the stability order is E□F□D□C□B□A for the structures at these performed theoretical levels.

Bond Dissociation Energies (BDE)

Bond dissociations investigation is essential and basic property for understanding the decomposition process of the High energy materials, since they are directly relevant to the stability and sensitivity of the high energy materials [21]. The energy required for bond hemolysis at 298.15 K temperature and 1 atmosphere pressure corresponds to the energy of reaction A-B → A° + B°, which is the bond dissociation energy of the compound A-B by definition. Therefore, the bond dissociation energy can be given in terms of follow equation:

$$BDE_{(A\text{-}B)} = E_{(A^{o})} + E_{(B^{o})} - E_{(A\text{-}B)} \qquad (2)$$

Where A-B corresponds for the structures, A^o and B^o stand for the corresponding product radicals after the bond dissociation, $BDE_{(A\text{-}B)}$ is the bond dissociation energy of bond A-B. The bond dissociation energy with ZPE correction can be calculated by follow equation:

$$BDE_{(A\text{-}B)ZPE} = BDE_{(A\text{-}B)} + \Delta ZPE \qquad (3)$$

The bond dissociation energies were calculated at the B3LYP/6-311G(d,p) level. Table 8 shows calculated total energies of tetrazine derivatives, fragments, NO_2 and NH_2 at the equilibrium geometries and resulting BDEs at mentioned level of theory. As seen from the table, the relative stability order of these structures may be in the order: F(6)□ B□ C(5)=C(6)□ F(5)□ D□ E(5)=E(6). It can be deduced that the BDEs for these molecules are highly substitution dependent. According to suggestion of Chung [22], the bond dissociation energy more than 20 kcal/mol corresponds for a compound to be considered as a viable candidate of high energy density material (HEDM). Therefore, we can conclude that the all molecules are viable candidate of HEDMs.

The frontier molecular orbital energies

Table 9 shows the HOMO and LUMO energies (ε) of the molecules computed at B3LYP/6-311G(d,p) level of theory. The frontier orbitals energies increase by increasing amino substituent and decrease by increasing the number of nitro substituent on the 1,2,3,4-tetrazine ring. These are general trends of electron withdrawing substituents which lower the frontier orbitals energy levels and electron donating substituents which higher the frontier orbitals energy levels. The order of energy gap values, that is the difference between the LUMO and HOMO energy levels, is C>B>A>E>D>F at the B3LYP/6-311G (d,p) level of theory. Figures 6 and 7 provide the frontier orbitals map.

Heats of formation, predicted densities and detonation of the structures

The heats of formation (HOF) values were calculated at B3LYP/6-311G (d,p) level and listed in the table 10. In this study, isodesmic reaction method is employed. In isodesmic reaction, the numbers of bonds and bond types are preserved on both sides of the reaction [23]. The accuracy of HOF obtained computationally is conditioned by the reliability of HOF of the reference compounds. The isodesmic reactions for HOF calculation are shown in Scheme 1.

For the isodesmic reactions, heat of reaction ΔH at 298 K can be calculated from the following equations:

$$\Delta H_{298} = \Sigma\Delta H_{f,P} - \Sigma\Delta H_{f,R} \qquad (4)$$

$$\Delta H_{298.15K}=\Delta E_{298.15K}+\Delta(PV)=\Delta E_0+\Delta ZPE+\Delta H_T+\Delta nRT= \Sigma\Delta H_{f\square,P} - \Sigma\Delta H_{f\square,R} \qquad (5)$$

where $\Delta H_{f,P}$ and $\Delta H_{f,R}$ are the heats of formation of products and reactants at 298 K, respectively. ΔE_0 and ΔZPE correspond to the total energy difference and the zero point energy difference between products and reactants at 0 K, respectively. ΔH_T is the changes in thermal correction to enthalpies between products and reactants. Δ(PV) equals ΔnRT for reaction in gas phase. For isodesmic reactions, Δn=0. As seen from the table, the HOF order is E□D□A□B□F□C for the structures at B3LYP/6-311G(d,p) level of theory

Furthermore, density (ρ), detonation velocity (D), and detonation pressure (P) are the important parameters to evaluate the explosive performances of high energy materials and can be predicted by the following empirical Kamlet-Jacob equations [24]:

$$D=1.01(NM^{1/2}Q^{1/2})^{1/2}(1+1.3\rho) \qquad (6)$$

$$P=1.558\rho^2NM^{1/2}Q^{1/2} \qquad (7)$$

Stoichiometric ratio			
parameters	$c \geq 2a+b/2$	$2a+b/2>c \geq b/2$	$b/2>c$
N	(b+2c+2d)/4MW	(b+2c+2d)/4MW	(b+d)/2MW
M	4MW/(b+2c+2d)	(56d+88c-8b)/(b+2c+2d)	(2b+28d+32c)/(b+d)
Q	(28.9b+94.05a+0.239ΔHf)/MW	[28.9b+94.05(c/2-b/4) +0.239ΔHf]/MW	(57.8c+0.239ΔHf)/MW

where D: detonation velocity in km/s, P: detonation pressure in GPa, ρ: density of a compound in g/cm^3, N: moles of gaseous detonation products per gram of explosive (in mol/g), M: average molecular weight of gaseous products (in g/mol), Q: chemical energy of detonation in kJ/g. Table 10 collects the predicted V, ρ, Q, D and P values of the structures. As seen from the table, the D and P order is E□F□A□D□C□B for the structures at B3LYP/6-311G(d,p) level of theory. It is noted that the D and P values gradually increase when the nitro groups increase. In a word, it shows that the introduction of nitro group more than amino group can improve the detonation properties of the structures. For RDX and HMX, experimental value of D and P are 8.75 km/s, 9.10 km/s and 34.70 GPa, 39.00 GPa, respectively. The RDX and HMX are the current standards for detonation behavior. Comparing these values with data of Table 10 shows molecule E can be an explosive.

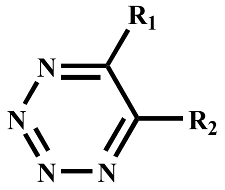

A: R_1=R_2=H **D: R_1=NO_2 , R_2=H**
B: R_1=NH_2 , R_2=H **E: R_1=R_2=NO_2**
C: R_1=R_2=NH_2 **F: R_1=NO_2 , R_2=NH_2**

Fig. 1. Molecular frameworks of studied compounds.

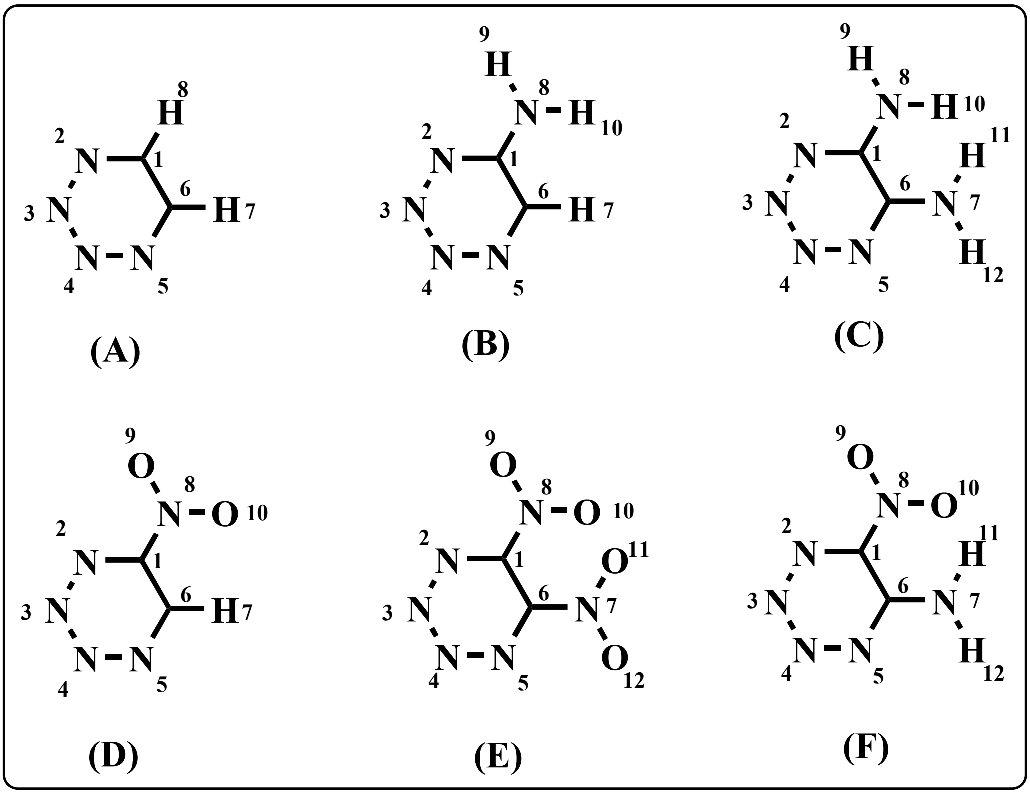

Fig. 2. The chemical structures and their atomic numbering.

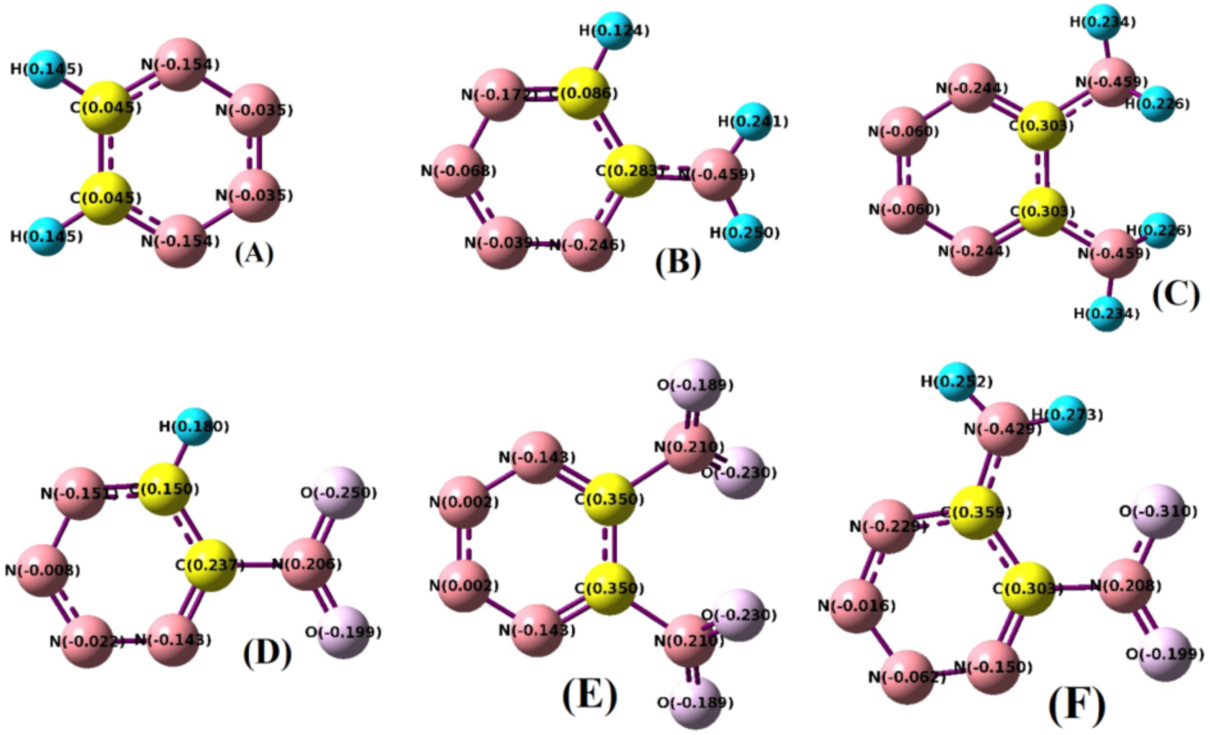

Fig. 3. The geometric structures of the molecules.

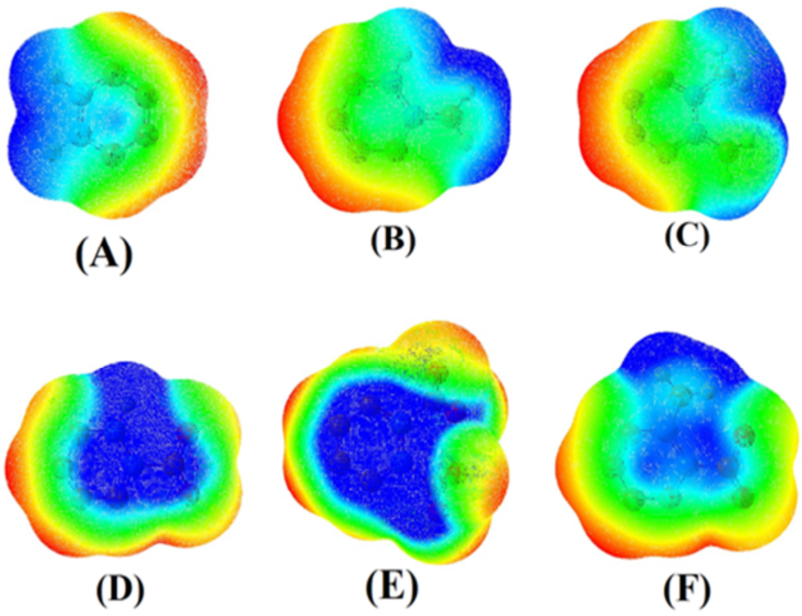

Fig. 4. The 3-D electrostatic potential maps of the structures.

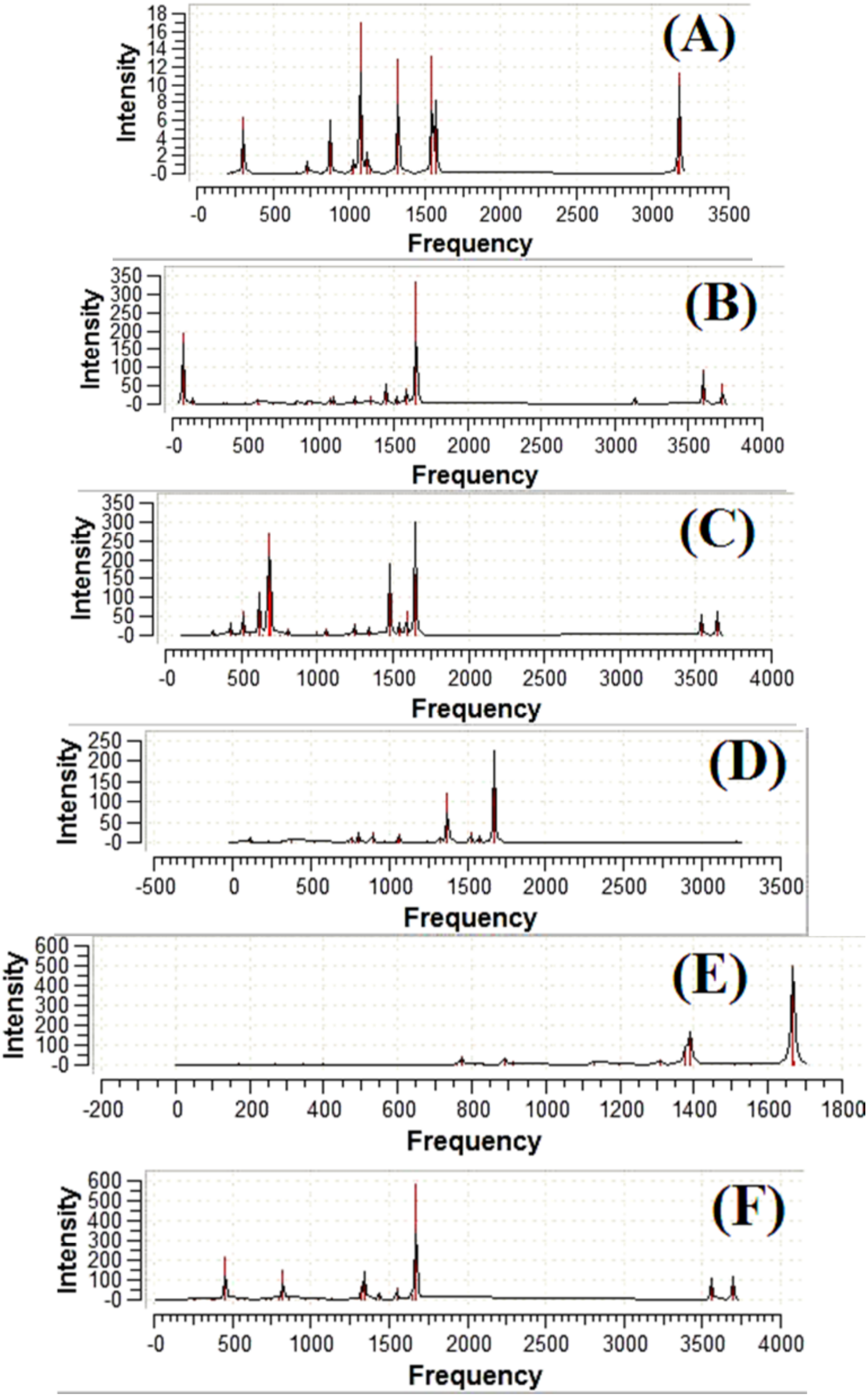

Fig. 5. The IR spectra of structures.

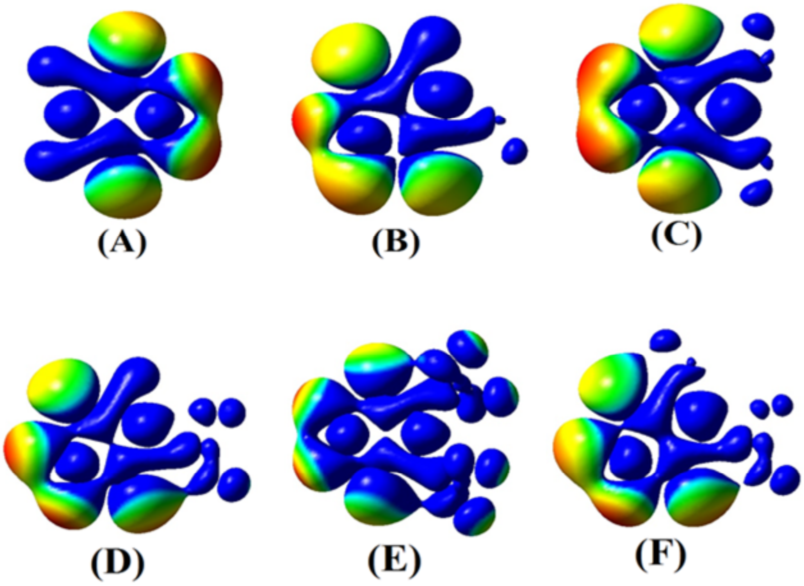

Fig. 6. HOMO orbital maps of structures.

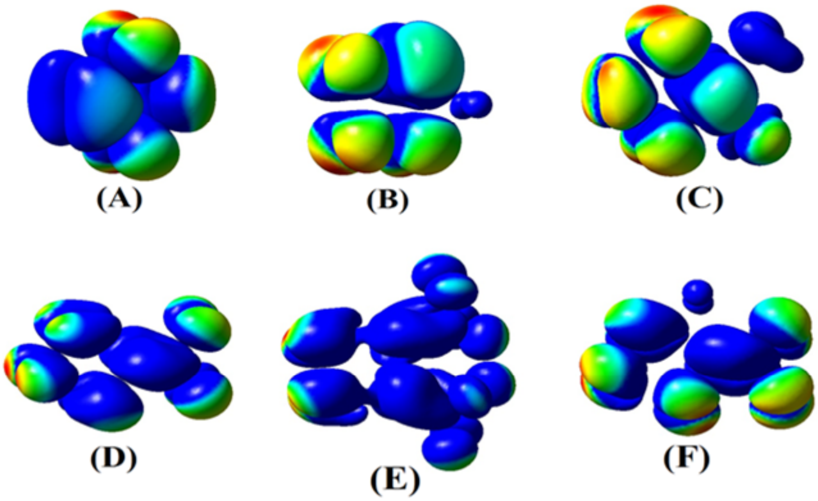

Fig. 7. LUMO orbital maps of structures.

$$Ar\text{-}NO_2 + CH_4 \longrightarrow Ar\text{-}H + CH_3NO_2$$

$$Ar\text{-}NH_2 + CH_4 \longrightarrow Ar\text{-}H + CH_3NH_2$$

Scheme 1. The isodesmic reactions for HOF calculations.

Table 1. Dipole moments of the structures

Structures	μ_X (Debye)	μ_Y (Debye)	μ_Z (Debye)	μ_{Tot} (Debye)
A	-4.6026	0.0001	0.0022	4.6026
B	6.4530	2.3556	0.0039	6.8695
C	7.1386	0.0000	0.0000	7.1386
D	0.3411	2.1901	0.0003	2.2165
E	-0.6771	0.0000	0.0000	0.6771
F	-0.7924	4.9636	0.0000	5.0265

Table 2. Bond lengths of structures calculated at B3LYP/6-311G(d,p) level

Bonds (A°)	A	B	C	D	E	F
C1-N2	1.324	1.338	1.317	1.305	1.306	1.305
N2-N3	1.336	1.326	1.346	1.339	1.340	1.322
N3-N4	1.313	1.308	1.298	1.312	1.305	1.335
N4-N5	1.337	1.347	1.346	1.333	1.340	1.299
N5-C6	1.324	1.310	1.317	1.326	1.305	1.362
C6-C1	1.392	1.412	1.423	1.389	1.392	1.411
C1-H7	1.085	-	-	-	-	-
C6-H8	1.084	1.087	-	1.082	-	-
C1-N7	-	1.348	1.374	1.508	1.494	1.494
C6-N8	-	-	1.374	-	1.494	1.332
N7-H9	-	1.009	1.012	-	-	-
N7-H10	-	1.004	1.012	-	-	-
N8-H11	-	-	1.011	-	-	1.009
N8-H12	-	-	1.012	-	-	1.009
N7-O9	-	-	-	1.209	1.208	1.206
N7-O10	-	-	-	1.223	1.218	1.235
N8-O11	-	-	-	-	1.219	-
N8-O12	-	-	-	-	1.207	-

Table 3. Bond angles of the structures calculated at B3LYP/6-311G(d,p) level

Bond angles (degree)	A	B	C	D	E	F
C1-N2-N3	118.138	118.736	119.239	117.555	118.521	120.560
N2-N3-N4	121.786	122.701	121.521	121.120	121.385	119.233
N3-N4-N5	121.752	120.587	121.522	122.157	121.355	122.670
N4-N5-C6	118.126	119.206	119.242	118.687	118.597	120.507
N5-C6-C1	120.074	120.153	119.121	118.068	120.042	115.711
C6-C1-N2	120.124	118.617	119.132	122.412	120.090	121.320
N2-C1-H7	116.865	-	-	-	-	-
N2-C1-N7	-	117.755	119.595	117.125	116.478	115.800
C6-C1-H7	123.011	-	-	-	-	-
C6-C1-N7	-	123.628	121.207	120.462	123.325	122.881
N5-C6-H8	116.860	117.174	-	118.6	-	-
N5-C6-N8	-	-	119.604	-	116.503	116.574
C1-C6-H8	123.066	122.673	-	123.332	-	-
C1-C6-N8	-	-	121.208	-	123.347	127.715
C1-N7-H9	-	118.347	113.410	-	-	-
C1-N7-H10	-	122.104	116.036	-	-	-
H9-N7-H10	-	119.549	113.942	-	-	-
C1-N7-O9	-	-	-	117.720	117.033	118.652
C1-N7-O10	-	-	-	114.776	114.148	115.483
O9-N7-O10	-	-	-	127.504	128.805	125.865
C6-N8-O11	-	-	-	-	114.133	-
C6-N8-O12	-	-	-	-	117.030	-
O11-N8-O12	-	-	-	-	128.821	-
C6-N8-H11	-	-	115.939	-	-	119.792
C6-N8-H12	-	-	113.333	-	-	117.666
H11-N8-H12	-	-	114.049	-	-	122.542

Table 4. Dihedral angles of the structures calculated at B3LYP/6-311G(d,p) level

Dihedral angles (degree)	A	B	C	D	E	F
N2-C1-N7-H9	-	-0.023	9.231	-	-	-
N2-C1-N7-H10	-	-179.839	143.951	-	-	-
C6-C1-N7-H9	-	179.917	-173.727	-	-	-
C6-C1-N7-H10	-	0.108	-39.007	-	-	-
N5-C6-N8-H11	-	-	143.947	-	-	179.986
N5-C6-N8-H12	-	-	9.251	-	-	0.055
C1-C6-N8-H11	-	-	-39.057	-	-	-0.052
C1-C6-N8-H12	-	-	-173.753	-	-	-179.981
N2-C1-N7-O9	-	-	-	-0.023	48.946	-0.035
N2-C1-N7-O10	-	-	-	179.946	-129.772	-179.976
C6-C1-N7-O9	-	-	-	-179.983	-134.811	179.969
C6-C1-N7-O10	-	-	-	3.256	46.471	0.028
N5-C6-N8-O11	-	-	-	-	-129.705	-
N5-C6-N8-O12	-	-	-	-	48.946	-
C1-C6-N8-O11	-	-	-	-	46.509	-
C1-C6-N8-O12	-	-	-	-	-134.840	-
N3-N2-C1-N7	-	-179.940	179.627	180.000	176.323	-180.000
N4-N5-C6-N8	-	-	179.578	-	176.300	-179.984
N5-C6-C1-N7	-	179.910	178.230	180.000	-175.672	180.000
N2-C1-C6-N8	-	-	178.275	-	-175.645	-179.992
C1-N2-N3-N4	-0.0450	-0.017	1.854	0.044	-0.749	-4.519
N2-N3-N4-N5	0.101	-0.014	-4.202	-2.190	1.173	2.238
N3-N4-N5-C6	-0.097	-4.927	1.859	-1.116	-0.750	-2.942
N4-N5-C6-C1	0.041	0.085	2.517	-3.464	-0.039	-2.396
N5-C6-C1-N2	2.240	-0.144	-4.715	0.062	0.440	-2.475
C6-C1-N2-N3	1.428	0.112	2.522	-0.078	-0.041	2.184

Table 5. NICS values for the structures calculated at B3LYP/6-311G(d,p) level

Structures	NICS(0)
A	-2.550
B	-2.119
C	-3.196
D	-5.567
E	-7.022
F	-5.540

Table 6. Calculated total energies (in a.u.) for the structures at spin-restricted Hartree-Fock (RHF) method with different basis sets

Structures	HF/6-31G(d,p)	HF/6-31+G(d,p)	HF/6-311G(d,p)	HF/6-311+G(d,p)	HF/cc-pvDZ
A	-294.514896	-294.522684	-294.575983	-294.581492	-294.538161
B	-349.547762	-349.558138	-349. 621529	-349.629142	-349.572912
C	-404.576959	-404.589800	-404.664091	-404.673572	-404.605349
D	-497.960135	-497.973909	-498.075075	-498.085602	-498.004613
E	-701.388034	-701.408824	-701.557271	-701.573546	-701.453783
F	-552.998703	-553.014537	-553.125876	-553.138209	-553.045119

The total energies are corrected for ZPVE.

Table 7. Calculated total energies (in a.u.) for the structures at B3LYP method with different basis sets

Structures	B3LYP/6-31G(d,p)	B3LYP/6-31+G(d,p)	B3LYP/6-311G(d,p)	B3LYP/6-311+G(d,p)	B3LYP/cc-pvDZ
A	-296.252452	-296.264260	-296.318774	-296.326246	-296.270963
B	-351.613034	-351.629365	-351.694905	-351.705149	-351.632713
C	-406.967852	-406.988366	-407.065040	-407.078100	-406.989546
D	-500.732724	-500.753496	-500.856371	-500.870318	-500.772925
E	-705.200475	-705.231149	-705.381948	-705.403223	-705.262364
F	-556.101597	-556.125868	-556.240089	-556.256295	-556.143172

The total energies are corrected for ZPVE.

Table 8. Calculated total energies of the structures, fragments, NH_2 and NO_2 at the equilibrium geometries and resulting bond dissociation energies (BDE)

Structures	Formula	Parent energy (hartrees)	Fragment energy (hartrees)	NO_2 energy (hartrees)	NH_2 energy (hartrees)	BDE (kcal/mol)
B	$C_2H_3N_5$	-351.69491	-295.65519	-205.12390	-55.87623	102.592
C(5)	$C_2H_4N_6$	-407.06504	-351.03727	-205.12390	-55.87623	95.093
C(6)	$C_2H_4N_6$	-407.06504	-351.03727	-205.12390	-55.87623	95.093
D	$C_2HN_5O_2$	-500.85637	-295.65519	-205.12390	-55.87623	48.494
E(5)	$C_2N_6O_4$	-705.38195	-500.18637	-205.12390	-55.87623	44.980
E(6)	$C_2N_6O_4$	-705.38195	-500.18637	-205.12390	-55.87623	44.980
F(5)	$C_2H_2N_6O_2$	-556.24009	-351.03727	-205.12390	-55.87623	49.523
F(6)	$C_2H_2N_6O_2$	-556.24009	-500.18637	-205.12390	-55.87623	111.377

Key to the notation: B(L) stands for the radical obtained from B structure by removing the functional group at position L.

CONCLUSIONS

In this study, stabilities of six structures as potential candidates for high energy density materials (HEDMs) have been investigated computationally by using quantum chemical treatment. Full geometrical optimizations of nitrogen-rich structures were performed using ab initio and density functional theory (DFT, B3LYP) at the levels of 6-31G(d,p), 6-31+G(d,p), 6-311G(d,p), 6-311+G(d,p), cc-pvDZ. Introduction of nitro and amino groups into 1, 2, 3, 5- tetrazine compound slightly affects the BDE and HOF. The detonation performance data are calculated according to the HOFs calculated by B3LYP/6-311G(d,p) level of theory and the values of D and P increase when the number of –NO2 group increases. Also, it concluded that the all structures are viable candidate of high energy density materials (HEDMs).

Table 9. The HOMO and LUMO energies of the structures calculated at B3LYP/6-311G(d,p) level

Structures	MOs number	HOMO orbital	HOMO (a.u.)	LUMO orbital	LUMO (a.u.)	Δε (a.u.)
A	120	21 (A)	-0.27229	22 (A)	-0.10803	0.16426
B	144	25 (A)	-0.25580	26 (A)	-0.08442	0.17138
C	168	29 (A)	-0.25396	30 (A)	-0.06564	0.18832
D	168	32 (A)	-0.30581	33 (A)	-0.15735	0.14846
E	216	43 (A)	-0.33218	44 (A)	-0.16984	0.16234
F	192	36 (A)	-0.28473	37 (A)	-0.14189	0.14284

$\Delta\varepsilon = \varepsilon_{LUMO} - \varepsilon_{HOMO}$

Table 10. HOFs, predicted densities and detonation properties of the molecules

Structures	OB_{100}	HOF (kJ/mol)	Q (kJ/g)	V (cm^3/mol)	ρ (g/cm^3)	D (km/s)	P (GPa)
A	-97.53	545.1	1463.348	48.688	1.685	7.992	27.207
B	-90.69	482.598	1188.606	69.504	1.396	7.005	18.433
C	-85.68	440.284	1135.586	80.567	1.391	7.124	19.016
D	-31.49	547.594	1813.294	86.367	1.471	7.710	23.161
E	0.00	581.760	1902.001	99.462	1.729	8.945	34.633
F	-33.80	467.269	1524.407	84.185	1.687	8.218	28.792

*Average valu from 100 single-point volume calculations at the B3LYP/6-311G(d,p) level.
Q: Heat of explosion, V: Volume of explosion, D: Velocity of detonation, P: Pressure of explosion.

REFERENCES

[1]. M. Mahkam, M. Nabati, A. Latifpour and J. Aboudi, Des. Monomers Polym. 17, (2014) 453.

[2]. M. Mahkam, Z. Namazifar, M. Nabati and J. Aboudi, Iran. J. Org. Chem. 6, (2014) 1217.

[3]. M. Nabati and M. Mahkam, Iran. Chem. Commun. 2, (2014) 164.

[4]. L. R. Ahar, M. H. Sadr, K. Zare and S. M. Tabatabei, J. Phys. Theor. Chem. IAU Iran. 11, (2014) 129.

[5]. W. C. Lothrop and G. R. Handrick, Chem. Revs., 44, (1949) 419.

[6]. M. Mahkam, H. R. Kafshboran and M. Nabati, Des. Monomers Polym. 17, (2014) 784.

[7]. M. Nabati and M. Mahkam, Iran. J. Org. Chem. 5, (2013) 1157.

[8]. A. Teymori, S. Amiri, B. Massoumi, M. Mahkam snd M. Nabati, Iran. J. Org. Chem. 6, (2014) 1287.

[9]. M. Nabati and M. Mahkam, J. Phys. Theor. Chem. IAU Iran. 12, (2015) 33.

[10]. M. Nabati and M. Mahkam, Iran. Chem. Commun. 2, (2014) 129.

[11]. M. Nabati, M. Mahkam and H. Heidari, Iran. Chem. Commun. 2, (2014) 236.

[12]. M. J. Frisch, G. W. Trucks, H. B. Schlegel, G. E. Scuseria, M. A. Robb, J. R. Cheeseman, J. A. Montgomery Jr., T. Vreven, K. N. Kudin, J. C. Burant, J. M. Millam, S. S. Iyengar, J. Tomasi, V. Barone, B. Mennucci, M. Cossi, G. Scalmani, N. Rega, G. A. Petersson, H. Nakatsuji, M. Hada, M. Ehara, K. Toyota, R. Fukuda, J. Hasegawa, M. Ishida, T. Nakajima, Y. Honda, O. Kitao, H. Nakai, M. Klene, X. Li, J. E. Knox, H. P. Hratchian, J. B. Cross, C. Adamo, J. Jaramillo, R. Gomperts, R. E. Stratmann, O. Yazyev, A. J. Austin, R. Cammi, C. Pomelli, J. W. Ochterski, P. Y. Ayala, K. Morokuma, G.A. Voth, P. Salvador, J. J. Dannenberg, V. G. Zakrzewski, S. Dapprich, A. D. Daniels, M. C. Strain, O. Farkas, D. K. Malick, A. D. Rabuck, K. Raghavachari, J. B. Foresman, J. V. Ortiz, Q. Cui, A. G. Baboul, S. Clifford, J. Cioslowski, B. B. Stefanov, G. Liu, A. Liashenko, P. Piskorz, I. Komaromi, R. L. Martin, D. J. Fox, T. Keith, M. A. Al-Laham, C. Y. Peng, A. Nanayakkara, M. Challacombe, P. M. W. Gill, B. Johnson, W. Chen, M. W. Wong, C. Gonzalez and J. A. Pople, Gaussian 03. Revision B.01. Gaussian Inc. Wallingford. CT. 2004.

[13]. S. H. Vosko, L. Wilk and M. Nusair, Can. J. Phys. 58, (1980) 1200.

[14]. C. Lee, W. Yang and R. G. Parr, Phys. Rev. B. 37, (1988) 785.

[15]. M. Nabati and M. Mahkam, Iran. J. Org. Chem. 6, (2014) 1331.

[16]. M. Vatanparast, N. Javadi, R. P. Talemi and E. Parvini, Iran. Chem. Commun. 2, (2014) 317.

[17]. L. Türker, J. Mol. Struct. 681, (2004) 15.

[18]. M. Mahkam, M. Nabati and H. R. Kafshboran, Iran. Chem. Commun. 2, (2014) 34.

[19]. H. Jiao and P. R. Schleyer, J. Phys. Org. Chem. 11, (1998) 655.

[20]. P. R. Schleyer, C. Maerker, A. Dransfeld, H. Jiao, and N. J. R. E. Hommes, J. Am. Chem. Soc., 118, (1996) 6317.

[21]. M. Nabati and M. Mahkam, Iran. J. Org. Chem. 6, (2014) 1397.

[22]. M. Nabati and M. Mahkam, Silicon, 8, (2016) in press.

[23]. L. Qiu, H. M. Xiao, X. H. Ju and X. D. Gong, Int. J. Quantum Chem. 105, (2005) 48.

[24]. M. J. Kamlet and S. J. Jacobs, J. Chem. Phys. 48, (1968) 23.